



<http://www.diva-portal.org>

This is the published version of a paper published in *Vehicle System Dynamics*.

Citation for the original published paper (version of record):

Kulkarni, R., Qazizadeh, A., Berg, M., Dirks, B., Ingemar, P. (2021)  
Investigating the effect of the equivalent conicity function's nonlinearity on the  
dynamic behaviour of a rail vehicle under typical service conditions  
*Vehicle System Dynamics*  
<https://doi.org/10.1080/00423114.2021.1962537>

Access to the published version may require subscription.

N.B. When citing this work, cite the original published paper.

Permanent link to this version:

<http://urn.kb.se/resolve?urn=urn:nbn:se:kth:diva-299580>



# Investigating the effect of the equivalent conicity function's nonlinearity on the dynamic behaviour of a rail vehicle under typical service conditions

Rohan Kulkarni, Alireza Qazizadeh, Mats Berg, Babette Dirks & Ingemar Persson

To cite this article: Rohan Kulkarni, Alireza Qazizadeh, Mats Berg, Babette Dirks & Ingemar Persson (2021): Investigating the effect of the equivalent conicity function's nonlinearity on the dynamic behaviour of a rail vehicle under typical service conditions, Vehicle System Dynamics, DOI: [10.1080/00423114.2021.1962537](https://doi.org/10.1080/00423114.2021.1962537)

To link to this article: <https://doi.org/10.1080/00423114.2021.1962537>



© 2021 The Author(s). Published by Informa UK Limited, trading as Taylor & Francis Group



Published online: 11 Aug 2021.



Submit your article to this journal [↗](#)





View related articles [↗](#)



View Crossmark data [↗](#)

# Investigating the effect of the equivalent conicity function's nonlinearity on the dynamic behaviour of a rail vehicle under typical service conditions

Rohan Kulkarni <sup>a</sup>, Alireza Qazizadeh <sup>a</sup>, Mats Berg <sup>a</sup>, Babette Dirks <sup>b</sup> and Ingemar Persson <sup>c</sup>

<sup>a</sup>Department of Engineering Mechanics, KTH Royal Institute of Technology, Stockholm, Sweden;

<sup>b</sup>Department of Technology & Environment, Swedish Transport Administration, Västertås, Sweden;

<sup>c</sup>AB DEsolver, Östersund, Sweden

## ABSTRACT

Generally, the equivalent conicity function (ECF) is denoted by equivalent conicity at 3mm ( $\lambda_{3\text{mm}}$ ) and a Nonlinearity Parameter (NP). NP describes the nonlinearity of the ECF and its influence on a vehicle design is explored thoroughly, however, NP's role in vehicle and track maintenance is not researched yet. This paper investigates the influence of track maintenance actions on vehicle dynamics with help of NP vs  $\lambda_{3\text{mm}}$  scatter plots of ECF database. The ECF database is constructed by combining measured worn wheel and rail profile pairs of the Swedish high-speed vehicle and rail network, respectively. The ECF database revealed an inverse relationship between  $\lambda_{3\text{mm}}$  and NP, i.e., NP is negative for larger  $\lambda_{3\text{mm}}$  values. The combination of negative NP and high  $\lambda_{3\text{mm}}$  causes reduction in the vehicle's nonlinear critical speed and vehicle often exhibit the unstable running on the Swedish rail network. Thus, the occurrence of ECF with negative NP and high  $\lambda_{3\text{mm}}$  is undesirable and the undesirable ECF can be converted into desirable ECF by grinding the rail, which converts ECF's into positive NP and low  $\lambda_{3\text{mm}}$  combinations. Thus, the NP parameter along with the  $\lambda_{3\text{mm}}$  must be considered in track maintenance decisions.

## ARTICLE HISTORY

Received 3 February 2021

Revised 25 June 2021

Accepted 24 July 2021

## KEYWORDS

Vehicle–track interaction;  
vehicle running instability;  
wheel–rail contact;  
equivalent conicity (EC);  
nonlinear parameter (NP);  
wheel and rail profile  
maintenance

## 1. Introduction

The present work is part of the project ‘A systematic approach to improve passenger ride comfort’ [1]. This collaboration project between the Swedish Transport Administration and train operator SJ AB, together with other partners, aims at improving the handling of poor ride comfort on-board passenger trains. The current rules and regulations are centred on safety and are often poorly adapted to handle ride comfort issues, especially for factors shared between infrastructure and rolling stock such as the wheel–rail contact conditions. The project is part of the IN2TRACK2 initiative [2] in the European research programme Shift2Rail.

**CONTACT** Rohan Kulkarni  [rohank@kth.se](mailto:rohank@kth.se)

© 2021 The Author(s). Published by Informa UK Limited, trading as Taylor & Francis Group

This is an Open Access article distributed under the terms of the Creative Commons Attribution-NonCommercial-NoDerivatives License (<http://creativecommons.org/licenses/by-nc-nd/4.0/>), which permits non-commercial re-use, distribution, and reproduction in any medium, provided the original work is properly cited, and is not altered, transformed, or built upon in any way.

One goal of the project is to find parameters describing the wheel–rail interface and their corresponding maintenance limits to ensure good ride comfort. An important parameter for the wheel–rail contact is the equivalent conicity (EC), etc. [3]. If the conicity is too high, the vehicle may suffer from bogie running instability. The EU Technical Specification for Interoperability (TSI) for locomotives and passenger rolling stock [4] and the TSI for infrastructure [5], put limits on the equivalent conicity value at 3 mm lateral wheelset displacement amplitude. However, the equivalent conicity is a function of the wheelset lateral displacement and just looking at its value at 3 mm amplitude is not sufficient. Therefore, a question has arisen if there are other parameters at the wheel–rail interface that play a decisive role for the running stability. Polach [6,7] showed that the forms of bifurcation, subcritical or supercritical, were mainly influenced by the nonlinearity of the wheel–rail contact function. He further proposed a nonlinearity parameter (NP) (Equation (1)) [7] to quantify the nonlinearity of the equivalent conicity function. The equivalent conicity function is categorized into type A and type B based on positive and negative values of NP, respectively:

$$NP = \frac{\lambda_{4mm} - \lambda_{2mm}}{2} \quad (1)$$

Mazzola et al. [8] also showed a similar influence of type A and type B equivalent conicity functions on the bifurcation behaviour of the ETR500 train through simulations. In further research, Polach showed that as the vehicle running distance increases, the equivalent conicity of the wheel–rail pair increases and NP decreases [9]. Increased equivalent conicity combined with a negative value of NP, etc. results in significantly reduced nonlinear critical speed of the vehicle. Wei et al. [10] and Xu et al. [11] also investigated the effect of NP on the dynamic behaviour of a Chinese high-speed vehicle and showed that negative values of NP result in a reduction of the nonlinear critical speed of the vehicle. Polach et al. [12] further showed that the vehicle bifurcation behaviour is highly influenced by NP than other parameters such as primary suspension, creep coefficient and friction coefficient. Thus, NP and EC (at 3 mm) are of great influence on the form of bifurcation and vehicle behaviour. All the above-mentioned articles investigate the NP from a vehicle design perspective but not from the perspective of a parameter which can be suitable in the vehicle and track maintenance procedures.

The objective of this work is to investigate the effect of NP on running instability from the standpoint of vehicle and track maintenance to avoid the emergence of vehicle instability (hunting) for in-service, etc. vehicle and ensure desirable ride comfort. In this investigation, a large database of nonlinear equivalent conicity functions corresponding to various track gauges is obtained by combining measured wheel profile pairs of the X2000 vehicle with measured rail profile pairs from the Swedish rail network. The effect of the equivalent conicity function's NP value on the running stability of the Swedish high-speed vehicle X2000 was investigated by two approaches: the nonlinear critical speed identification and the safety limit method, described in the EN14363 [13] standard under typical service conditions. It was found that the high equivalent conicity in combination with a negative NP value was the primary reason behind poor vehicle–track interaction which resulted in deteriorated ride comfort. This research work underlines the importance of formulating limit values for equivalent conicity and NP to avoid unfavourable vehicle–track

interaction *and* this work further suggests vehicle and track maintenance actions (limit values, etc.) to reduce the risk of vehicle instability (hunting) for in-service vehicles.

## 2. Vehicle dynamic simulations

Vehicles seldom exhibit hunting in service, as unstably running vehicles is considered a safety risk. Therefore, hunting behaviour of the vehicle is investigated by means of the commercial multibody dynamics software GENSYS [14] by performing time-domain simulations. It is also easy to control the parameters influencing the vehicle stability inside GENSYS. In GENSYS, there are different ways for modelling wheel–rail contact. In this study, it is modelled as linear high stiffness spring and the FASTSIM algorithm is used to calculate creep forces using a lookup table [15]. The wheel–rail contact model allows for two simultaneous contact points. The wheel–rail contact geometry functions are calculated using a pre-processor in GENSYS, including the equivalent conicity functions calculated in accordance with the EN15302:2008 standard.

### 2.1. Multibody dynamic model

#### 2.1.1. Vehicle model

The Swedish train operator SJ operates the high-speed trains X2000 on the Swedish rail network. Most SJ X2000 trains consist of a power car, five intermediate coaches and a driving trailer and are operating at a top speed of 200 km/h. An intermediate coach is studied here [16]. The vehicle model consists of a carbody, two bogie frames and four wheelsets which are modelled as 6 DOF rigid bodies and are connected by the primary and secondary suspension elements. The primary and secondary suspension consists of spring and viscous damper elements in the  $x$ ,  $y$  and  $z$ -directions. Since X2000 coach is specifically designed to run on a track with high cant deficiencies, the primary suspension is relatively soft to give the wheelsets improved radial self-steering capabilities. The X2 coach model is also equipped with four yaw dampers i.e. two per bogie, which works in the longitudinal direction. The vehicle data are mainly confidential, but some data are shown in Table 1 and the static axle loads are 118.1 kN for all wheelsets.

#### 2.1.2. Track model

The track model consists of four massless masses, i.e.  $ral\_l$  and  $ral\_r$  (left and right rail),  $trc$  (track) and  $grd$  (ground). The mass  $trc$  is connected via spring-damper to fixed mass  $grd$  and has degree of freedom in lateral direction. The spring-damper coupling refers to the lateral stiffness of the ballast and soil. The rail masses,  $ral\_r$  and  $ral\_l$  have vertical and lateral degrees of freedom. The rails are connected to the track via the springs-damper

**Table 1.** Parameters of Eurofima and X2000 coach model [16].

Coach	Component	Mass (kg)	Mass moment of inertia			Height of mass centre above track plane (m)
			$J_{xx}$ (kgm <sup>2</sup> )	$J_{yy}$ (kgm <sup>2</sup> )	$J_{zz}$ (kgm <sup>2</sup> )	
X2000	Carbody	32,000	64,446	1,519,965	1,519,965	2
	Bogie	5500	3000	6000	8000	0.7
	Wheelset	1300	750	250	750	0.5

system, which represents flexibility provided by track assembly components in vertical and lateral directions [16].

## 2.2. Wheel-rail contact geometry

The equivalent conicity calculation of shortlisted worn wheel profiles in pair with nominal rail profile 60E1i30 [17] is formed and the results are plotted in scatter plots where the X-axis is  $\lambda_{3\text{mm}}$ , etc. and the Y-axis is NP. It is observed in the results shown in Figure 1 that NP is negative for wheel pairs with high  $\lambda_{3\text{mm}}$  for a track gauge of 1435 and 1437.5 mm. The scatter plots also show that the NP values corresponding to wheel pairs with  $\lambda_{3\text{mm}}$  higher than 0.4 are negative and the NP values reduce furthermore with the increase in equivalent conicity ( $\lambda_{3\text{mm}}$ ). Negative NP combined with  $\lambda_{3\text{mm}}$  greater than 0.4 increases the risk of the vehicle running unstable during regular service operation. The objective of this investigation is to investigate the effect of NP on dynamic stability of the vehicle during regular operation. Hence, two pairs of measured wheel profiles were selected such that both pairs of wheel profiles have  $\lambda_{3\text{mm}}$  greater than 0.4, while one wheel profile pair with positive NP (type A) and the other wheel profile pair has negative NP (type B). These two-wheel profiles are labelled T19 and T33 and their respective  $\lambda_{3\text{mm}}$  and NP values are shown as solid green (grey on greyscale) squares in the top scatter plot of Figure 1.

The shape of these two worn wheel profiles is compared against the wheel profile S1002t31 mm [18] in Figure 2, where lateral coordinate ( $Y$ ) is on the  $x$ -axis, whereas vertical coordinate ( $Z$ ) is on the left  $y$ -axis. Both wheel profiles are not very different from each other in the wheel flange region and have similar flange thickness and flange height measurements. Figure 2 also shows the wear depth of the wheel tread in dashed lines where the wear depth scale is on the right  $y$ -axis. Here, it is observed that both wheel profiles exhibit hollow tread wear. The wear depth of type A wheel profile is much lower than the wear depth of type B wheel profile and these two wear depth curves differ a lot from  $-20$  mm on the  $x$ -axis.

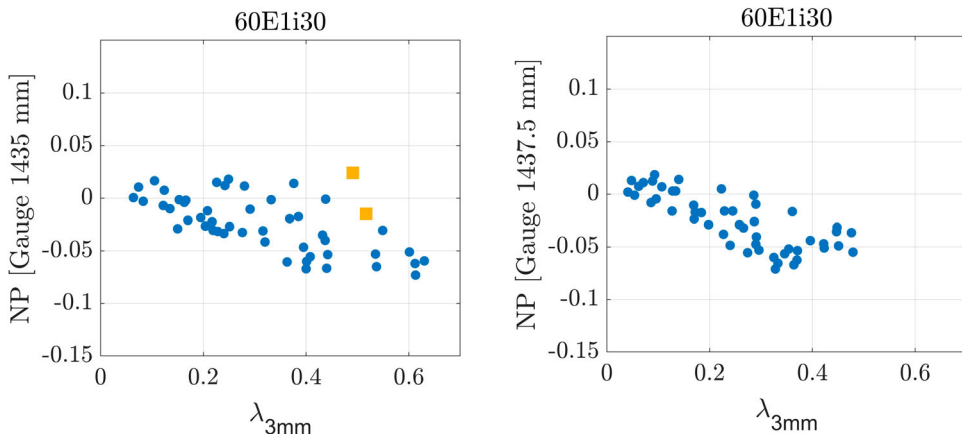


**Figure 1.** Scatter plot between equivalent conicity at 3 mm and NP of worn wheel profiles paired with nominal rail profile 60E1i30.

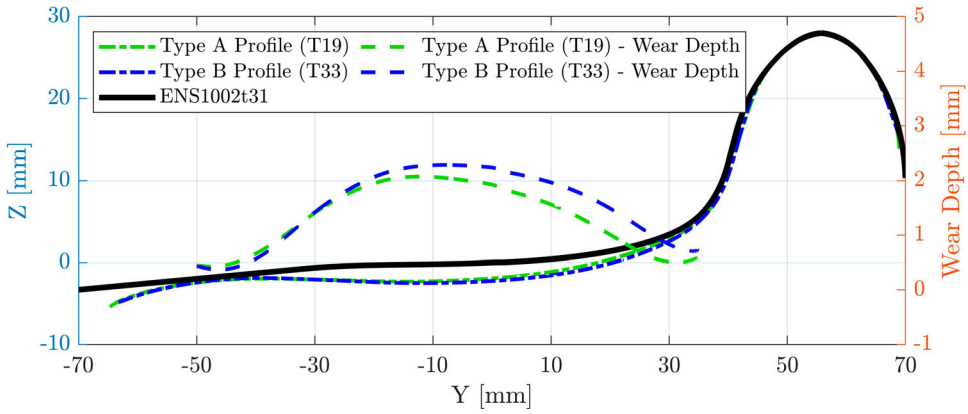


**Figure 2.** Geometry of shortlisted wheel profiles and tread wear depth.

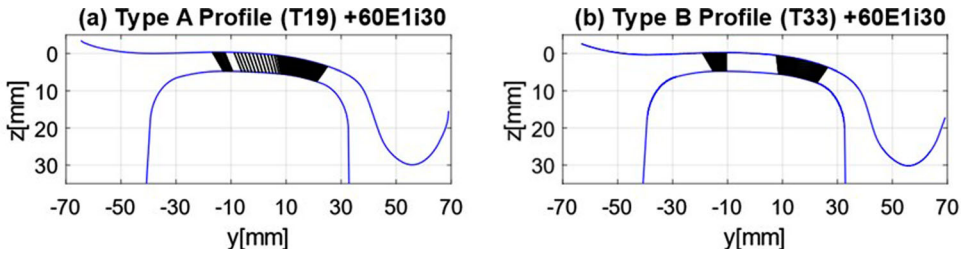


**Figure 3.** The contact point plots of Type A and Type B wheel profiles in combination with rail profile 60E1i30 for  $\pm 4$  mm lateral displacement of the wheelset with respect to track.

The calculation of wheel–rail contact geometry functions of the above-shown wheel profiles in combination with the nominal rail profile is performed in GENSYS. Wheel and rail contact point plots of both profiles are shown in Figure 3; where subfigures (a) and (b) correspond to type A and B profiles. In both subfigures lateral and vertical coordinates of the profiles are on the  $x$  and  $y$  axis, respectively; wheel and rail profiles are shown by blue (black on greyscale) curves. The contact point plot for  $\pm 4$  mm lateral wheelset displacement on track is produced where the wheel's contact point is connected to respective contact point on rail by black lines. It is observed in Figure 3(a) that the contact points of type A wheel profile exhibit gradual transition from rail head to gauge corner, whereas the contact points of type B profile suddenly jump from the top of the rail head towards the gauge corner, as shown in Figure 3(b).

The equivalent conicity function calculated in accordance with EN 15302:2008 for the track gauge of 1435 mm is shown in Figure 4. The black dashed line shows  $Y = 3$  mm, i.e. 3 mm lateral displacement of wheelset relative to the rail. The blue (black on greyscale) curve corresponds to type B ( $NP < 0$ ) wheel profiles, whereas the green (grey on greyscale) curve corresponds to type A ( $NP > 0$ ). The equivalent conicity function of these two-wheel profile pairs exhibits very similar equivalent conicity values for wheelset lateral displacement amplitude greater than 3 mm, but the slopes of the equivalent conicity functions around 3 mm are different. As the contact point suddenly shifts from rail head top to gauge corner for type B profile, the blue (black on greyscale) curve decreases rapidly for

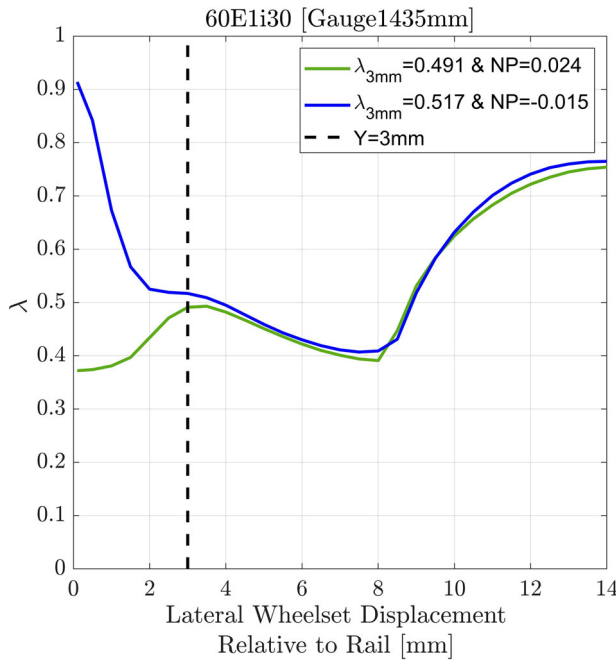


**Figure 4.** Equivalent Conicity function of the shortlisted wheel profiles.

amplitudes smaller than 3 mm and has an NP of  $-0.015$ . This is quite the opposite for type A, as the contact point gradually shifts from rail head to gauge corner; the green (grey on greyscale) curve increases for amplitudes smaller than 3 mm and has a positive NP.

### 2.3. Vehicle running instability investigation

The running stability of the X2000 vehicle model is investigated according to two methods [6] to understand the effect of NP on the running stability of the vehicle. The simulation setting is explained henceforth.

#### 2.3.1. Nonlinear critical speed identification

In the first method, bifurcation diagram is generated by numerical simulation with initial disturbance followed by parameter sweep [6]. The simulation is initiated at a vehicle speed much higher than the operating speed with an initial excitation to the vehicle followed by an ideal track (without irregularities). The speed of the vehicle is continuously decreased with very small speed reduction and the amplitude of the leading wheelset lateral oscillation is monitored continuously. The speed at which the wheelset's lateral oscillation damps out is taken as the nonlinear critical speed of the vehicle. In this investigation, the lateral oscillations of the leading wheelset are considered completely damped after the oscillation amplitude reduces below 0.5 mm because oscillations below 0.5 mm are barely noticeable in the carbody. The parameter setting of the simulation is listed below.

- (1) Initial excitation: A large excitation in lateral and yaw direction is applied to the centre of gravity of the carbody.



- (2) Track gauge: 1435 mm
- (3) Vehicle speed: 400 km/h with speed reduction of (1 km/h)/s
- (4) Wheel–rail friction coefficient = 0.5
- (5) Output signal: Lateral displacement of a leading wheelset
- (6) All wheels have the same wheel profile, i.e. either T19 or T33

### 2.3.2. Safety criteria method

The second method used for the investigation of the vehicle stability is the simplified measuring method defined in EN 14363:2016 [13], which uses the lateral acceleration on the bogie frame. The investigated signal is filtered and processed the same way as the sum of the guiding forces (bandpass filter, root mean square (RMS) value over 100 m distance with steps of 10 m) and should be compared with the limit value ( $\ddot{y}_{\text{lim}}^+$ ) specified as a function of bogie mass ( $m^+$ ) in tons as Equation (2). Multiple simulations are performed for constant speed varying from 150 to 400 km/h with a speed increment of 10 km/h. During all simulations, wheel–rail dry friction condition is assumed and a friction coefficient of 0.5 is selected.

$$\ddot{y}_{\text{lim}}^+ = \frac{1}{2} \left[ 12 \text{m/s}^2 - \frac{m^+}{5t} \text{m/s}^2 \right] = 5.19 \text{m/s}^2 \quad (2)$$

The simulation settings are explained as follows:

- (1) Selection of track irregularities:

The measured irregularities from 28 to 30 km on the Swedish track section number 354 (BDL354) are used for the stochastic excitation of the vehicle. This 2 km long section was selected because of the availability of measured rail profiles at the 28.859 km position marker and a poorer track quality relative to the other sections of BDL354. The Alignment Level (AL), Longitudinal Level (LL) and Cross Level (CL) irregularities are used in the simulation without scaling. Track Gauge (TG) irregularities are down-scaled to 10% to preserve the nature of both equivalent conicity functions at 1435 mm track gauge (Figure 4). The spatial distributions of the four track irregularities are shown in Figure 5.

The quality of the track irregularities of the shortlisted section is evaluated according to methodology and limits defined in EN 13848 [19]. The track section does not have any isolated track irregularity defects in AL, LL, CL, and TG irregularities. LL irregularities are mainly in Class B and Class C. AL irregularities are equally distributed in Classes A, B and C. CL irregularities of the selected track section are poor where most of the track is in Class D with some parts in Class E, which indicates the need for maintenance.

- (2) Running equivalent conicity distribution

The running equivalent conicity is calculated using the two equivalent conicity functions described above. In the calculation, it is assumed that the rail profiles are considered constant along the track and only the slight variation in track gauge is considered as a variable. The running conicity along the track section is shown in Figure 6. The top half of the figure shows the equivalent conicity at 3 mm where the green (grey on greyscale) curve shows the running conicity of the type A ( $\text{NP} > 0$ ) equivalent conicity function and blue

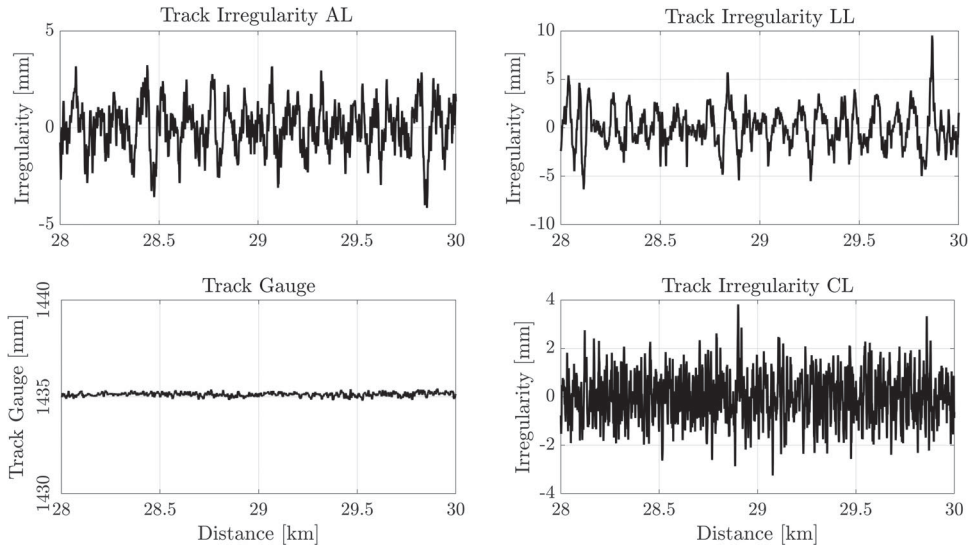


**Figure 5.** Spatial distributions of the four track irregularities.

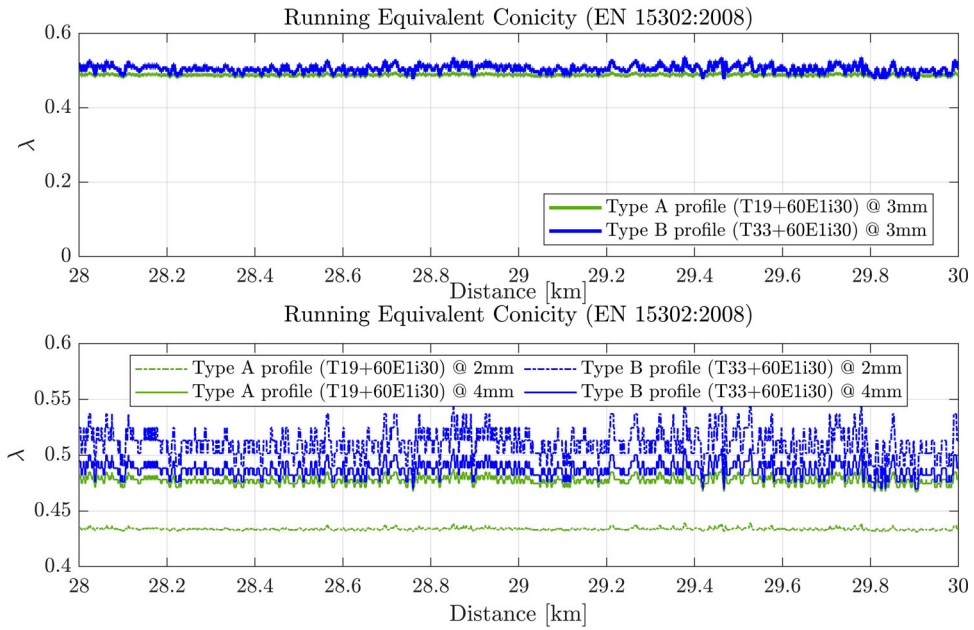


**Figure 6.** Running equivalent conicity distributions.

(black on greyscale) curve corresponds to the type B ( $NP < 0$ ) equivalent conicity function. It can be observed in the plot that the red and blue curves show almost constant equivalent conicity values along the track section.

The bottom half of Figure 6 shows the running equivalent conicity at 2 and 4 mm for both wheel profiles. It can be observed that the equivalent conicity at 4 mm for the wheel profiles is very similar, as shown by green and blue (grey and black on greyscale) solid

curves. It is also interesting to note that there is a significant difference in the equivalent conicity at 2 mm for the wheel profiles, as seen in green and blue (grey and black on greyscale) dash-dot curves. The equivalent conicity at 2 mm for type A ( $NP > 0$ ) is much lower than that of type B ( $NP < 0$ ).

### 3. Basic results

#### 3.1. Nonlinear critical speed identification

The results obtained by performing nonlinear critical speed identification of the X2000 vehicle is shown in Figure 7. In this figure, the lateral wheelset oscillation amplitude of the leading wheelset is plotted against the vehicle speed in the speed range of 180–350 km/h for simplicity. The green (grey on greyscale) and blue (black on greyscale) curves correspond to type A and type B equivalent conicity functions, respectively.

In the beginning of the simulation of type A equivalent conicity, the leading wheelset of the X2000 vehicle starts with steady-state lateral oscillations with an amplitude of 6 mm at the vehicle speed of 350 km/h. The amplitude of this lateral oscillation decreases gradually as the vehicle speed is reduced till 276 km/h. The amplitude of the lateral wheelset oscillations suddenly drops to 0 at 275 km/h and thus wheelset oscillations stop. This is a typical example of subcritical bifurcation behaviour of the vehicle and this subcritical bifurcation is attributed to the presence of type A equivalent conicity [6,7,9,12]. The lateral oscillations of the leading wheelset of the X2000 vehicle model with type B equivalent conicity function start with a steady-state solution of lateral wheelset oscillation with an amplitude of 5 mm. The amplitude of this lateral oscillation reduces gradually as the vehicle speed is reduced

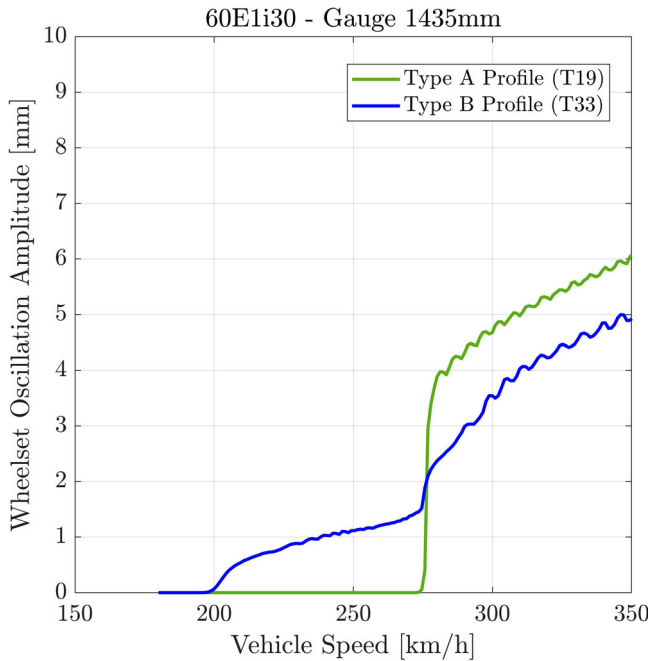


**Figure 7.** Subcritical and Supercritical bifurcation of the X2000 vehicle model.

and continues to reduce to very small amplitudes. The oscillations of the leading wheelset are considered completely damped after it reduces below 0.5 mm which occurs at a vehicle speed of 213 km/h. This is a typical example of supercritical bifurcation behaviour of the vehicle caused by the presence of type B equivalent conicity function [6,7,9,12].

The difference between the bifurcation behaviour of the X2000 vehicle model in the presence of type A and type B equivalent conicity function is distinctively visible in Figure 7. The type B equivalent conicity function reduces the nonlinear critical speed of the vehicle to 213 km/h which is significantly less than the nonlinear critical speed of 275 km/h obtained in the presence of type A equivalent conicity function. In the vehicle speed range of 213 to 275 km/h, type B equivalent conicity function generates higher wheelset oscillation amplitudes whereas this behaviour reverses above a vehicle speed of 275 km/h.

### 3.2. Safety criteria method

The main results of the vehicle running instability investigation in accordance with the safety criteria method are shown in Figure 8 which shows the variation in normalized lateral bogie frame acceleration against vehicle speed. The virtual accelerometer is mounted on the left-rear end of the leading bogie frame to record acceleration in each simulation, because the bogie frame's rear end is more sensitive to the instability than the front end. Bogie frame acceleration is post-processed in accordance with the simplified measurement scheme described in EN 14363:2016 [13]. The ordinate of Figure 8 is the maximum value of RMS of bandpass-filtered lateral bogie frame acceleration normalized with respect to the corresponding limit value defined by Equation (3). In Figure 8, green (grey on greyscale) bars correspond to bogie frame acceleration in the presence of type A equivalent conicity function and blue (black on greyscale) bars correspond to bogie frame acceleration in

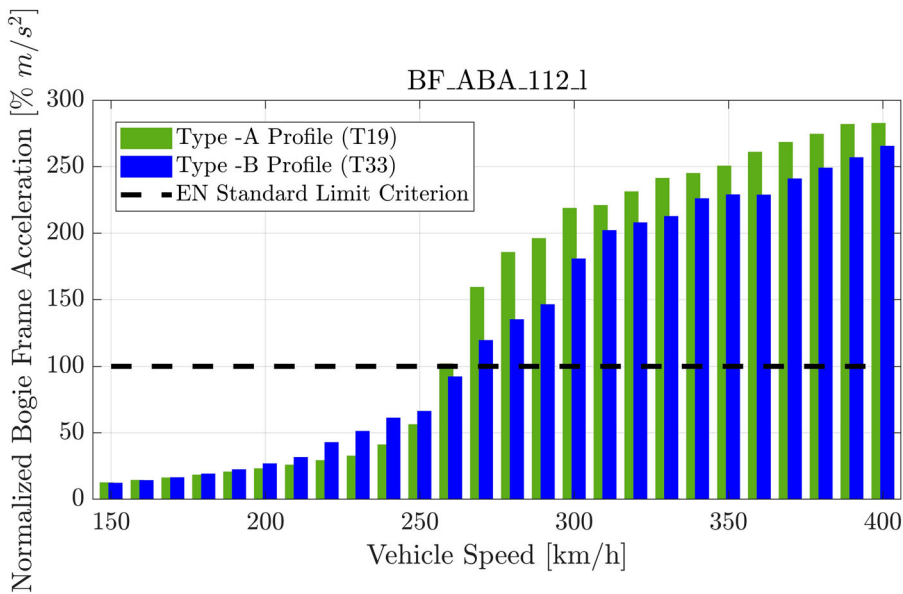


**Figure 8.** Lateral bogie frame acceleration vs. speed for two wheel profiles.

the presence of type B equivalent conicity function, whereas the limit value is shown by a dashed black line. The acceleration values are normalized by the limit value.

In Figure 8, it is observed that the blue (black on greyscale) and green (grey on greyscale) bars have the same height in the vehicle speed range of 150–170 km/h. After 180 km/h, the blue (black on greyscale) bars start rising faster than the green (grey on greyscale) bars and this phenomenon continues till 250 km/h. But suddenly the green (grey on greyscale) bars start rising faster and becomes greater than the blue (black on greyscale) bars after 260 km/h. It is also observed in the plot that both bar types cross the limit criteria close to 260 km/h, hence the vehicle's critical speed is 260 km/h based on the simplified method. The presence of type B equivalent conicity function induces the phenomena observed in the speed range of 180–250 km/h.

A spatial domain representation of both bars corresponding to 200 km/h vehicle speed in Figure 8 is presented in the adjoining Figure 9. In this plot, the green (grey on greyscale) curve corresponds to type A equivalent conicity function and the blue (black on greyscale) curve corresponds to type B equivalent conicity function. Both curves follow each other closely along the travel distance; however, the global maximum of the blue (black on greyscale) curve is higher than the global maximum of the green (grey on greyscale) curve which occurs around the 29 km position marker. This increase in RMS of the lateral bogie frame acceleration is the effect of the presence of type B equivalent conicity function at the wheel–rail interface. This difference increases rapidly in the vehicle speed range 180–250 km/h, as noticed in Figure 8.

In Figure 10, unfiltered lateral acceleration signals of the axlebox and bogie frame of the X2000 vehicle model running at a vehicle speed of 200 km/h are presented to highlight the effect of type A and type B equivalent conicity functions. The time signals represent a 250 m travel distance starting from 29 km. In all four plots, green (grey on greyscale) and blue (black on greyscale) curves correspond to vehicle behaviour in the presence of type A and type B equivalent conicity function, respectively. The top-left and top-right plots of Figure 10 show unfiltered lateral acceleration signals of leading wheelset left axlebox in time and frequency domain, respectively. The axlebox acceleration in the presence of type B profile (blue (black on greyscale) curve) exhibits higher amplitude due to the emergence of peaks

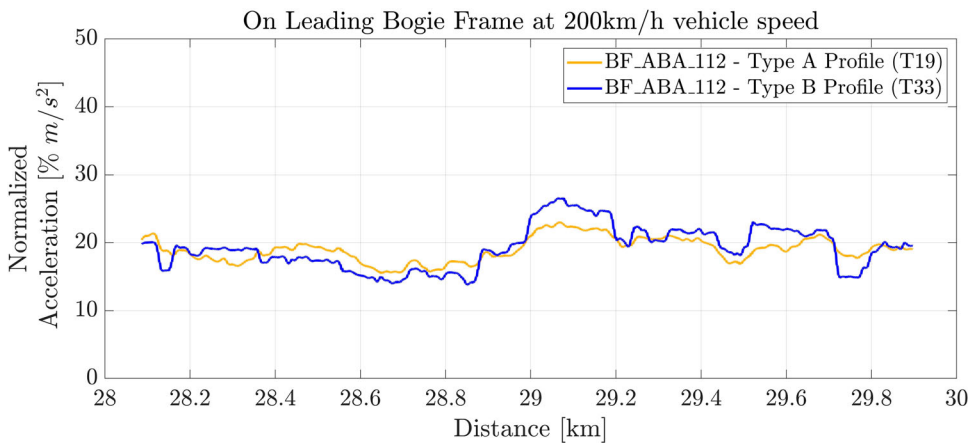


**Figure 9.** Moving RMS of bandpass-filtered lateral bogie frame acceleration.

## Raw Accelerations above Trailing Wheelset on Leading Bogie

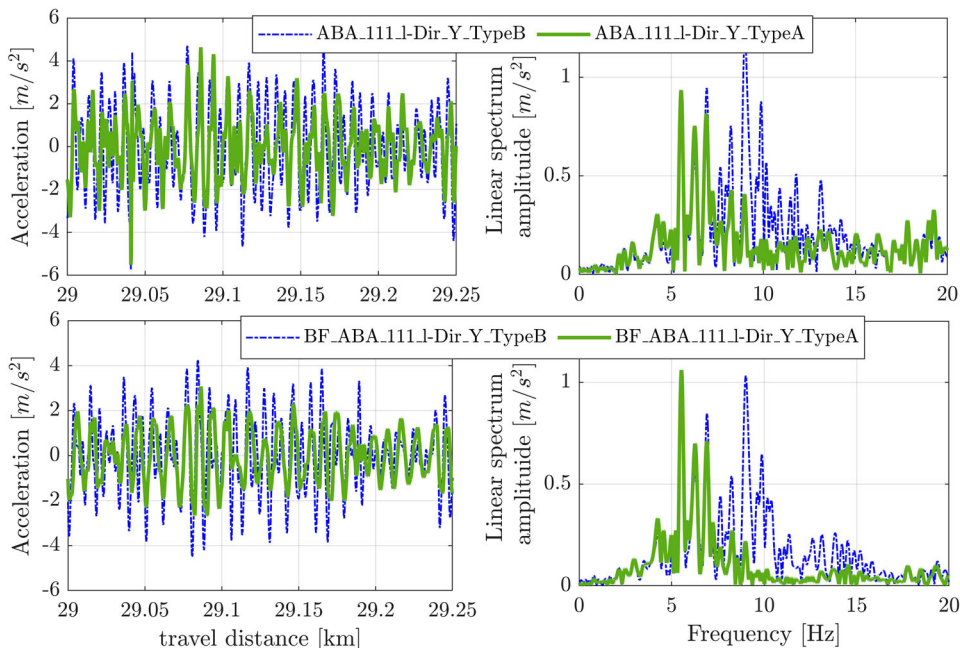


**Figure 10.** Unfiltered lateral acceleration signals of axlebox (top) and bogie frame (bottom) of X2000 at a speed of 200 km/h.

in frequency range 7–15 Hz in comparison with the green (grey on greyscale) curve and the same behaviour is reflected in the frequency domain representation. The green (grey on greyscale) and blue (black on greyscale) curves follow each other well in the frequency range of 0–7 Hz and 15–20 Hz, respectively; however, the blue (black on greyscale) curve has peaks at 9 and 10 Hz which are missing in the green (grey on greyscale) curve. These two peaks appear due to the small amplitude hunting behaviour caused by the presence of type B equivalent conicity function, which do not appear in the axlebox acceleration in the presence of type A equivalent conicity function.

The bottom-left and bottom-right plots of Figure 10 show the unfiltered lateral acceleration signals of the leading bogie frame (at a point above the trailing wheelset) in the spatial and frequency domain, respectively. The results are like the ones of axlebox acceleration explained above.

The results obtained by performing similar investigations for worn rail profiles measured on the BDL354 and BDL416 track sections are summarised in Table 2. The table shows the names of rail and wheel profiles followed by equivalent conicity at 3 mm ( $\lambda_{3\text{mm}}$ ), NP and type of equivalent conicity function. The results of vehicle running instability simulations by both methods are tabulated under the critical speed column. The column (i) lists the nonlinear critical speed obtained from the nonlinear dynamics-based method, i.e. bifurcation diagram. Column (ii) shows the vehicle's critical speed in accordance with the safety limit method (accelerations) and Column (iii) presents the vehicle speed at which bogie frame accelerations exceeds half of the safety limit (Equation (2)). Only the half



**Table 2.** Summarised results of vehicle running instability investigation.

Rail profile	Wheel profile	Eqv. conicity ( $\lambda_{3mm}$ )	NP value	Eqv. conicity function Type	Critical speed [km/h]		
					Bifurcation diagram (i)	$\ddot{y}_{lim}^+$ (ii)	$\ddot{y}_{lim}^+ / 2$ (iii)
60E1130	T19	0.49	0.024	A	275	260	250
	T33	0.50	−0.015	B	213	260	230
Bdl354 @28km	T19	0.48	−0.005	B	273	260	250
	T33	0.47	−0.03	B	213	260	230
Bdl354 @10km	T19	0.21	0.14	A	> 350	350	330
	T33	0.002	0.05	A	> 350	> 350	> 350
Bdl416 @139km	T19	0.48	−0.01	B	280	270	250
	T33	0.3	0.13	A	> 350	320	300
Bdl416 @177km	T19	0.58	−0.05	B	233	240	230
	T33	0.57	0.03	A	283	270	240
Bdl416 @180km	T19	0.57	−0.07	B	215	240	220
	T33	0.53	−0.03	B	275	270	250

of the safety limit is considered here because the safety limit acceleration is appropriate for dynamic safety certification of the vehicle but inappropriate to reveal deteriorated ride comfort due to vehicle instability occurrences.

It can be observed from the critical speed values given in Column (i) that the X2000 vehicle model exhibits supercritical bifurcation in the presence of type B equivalent conicity function and subcritical bifurcation in the presence of type A equivalent conicity function. There is a significant effect of the NP on the critical speed identified by the first two methods, as seen in Column (i) and (ii). It can be observed after the comparison of Column (i) and (ii) that there is a good agreement between the obtained results by both methods, but there are a few cases where a significant difference between critical speeds is observed. Such an example is described above. The Column (iii) is generated by identifying when the bogie frame acceleration exceeds 50% of the safety limit. It is observed in Column (iii) that the simulations in the presence of type B equivalent conicity function exceed the 50% limit much earlier than the simulations in the presence of type A equivalent conicity function. All entries in Table 2 are categorised in three groups based on their  $\lambda_{3mm}$  values. Group 1 contains entries which have  $\lambda_{3mm}$  values around 0.48 and these rows are shaded in a light olive green colour. Group 2 contains entries which have  $\lambda_{3mm}$  values around 0.57 and these rows are shaded in a light blue colour. Group 3 contains entries which cannot be grouped into a single group based on  $\lambda_{3mm}$  value and these rows are unshaded.

Group 1 entries contain both type A and type B equivalent conicity functions and the X2000 vehicle in two cases exceeds 50% of the safety limit earlier in the presence of type B than in the presence of type A equivalent conicity function. At the same time, it should be noted that this effect is not very pronounced when NP values are very close to zero. Nevertheless, the occurrence of supercritical bifurcation due to the presence of type B equivalent conicity function results in higher levels of lateral bogie frame accelerations. Group 2 entries also contain both type A and type B equivalent conicity functions and the X2000 vehicle exceeds 50% of the safety limit earlier in the presence of type B than in the presence of type A equivalent conicity function. It is very important to note that this sudden change from subcritical bifurcation to supercritical bifurcation based on equivalent conicity function can occur in service operation of the X2000 vehicle.

## 4. Further results and discussions

The purpose of this section is to discuss the effect of type A and type B equivalent conicity functions on the dynamic behaviour of the X2000 vehicle model while simulated on track sections BDL354 and BDL416.

### 4.1. BDL354

Scatter plots of equivalent conicity at 3 mm and NP for 54 pairs of measured wheel profiles in combination with measured rail profiles of BDL354 are shown in Figure 11, each scatter plot thus containing 54 markers. This figure is organised as Figure 1 where the top and bottom rows are presenting scatter plots for the track gauge of 1435 and 1437.5 mm, respectively. The first column corresponds to the nominal rail profile, i.e. 60E1i30 (the same as Figure 1), whereas the second and third columns correspond to the measured rail profiles of BDL354 at the position marker of 10.3277 km and 28.859 km, respectively. The important difference between these two measured rail profiles is that rail profile grinding is performed in the vicinity of 10.3277 km, whereas rail profile milling is performed in the vicinity of 28.859 km.

It is observed in both figures corresponding to 60E1i30 that the 54 wheel profile pairs exhibit  $\lambda_{3\text{mm}}$  values in the range of 0–0.7 and NP values in the range of  $-0.1$ – $0.05$ . Moreover, it is also observed that the NP value decreases from 0.05 to  $-0.1$  as the  $\lambda_{3\text{mm}}$  value

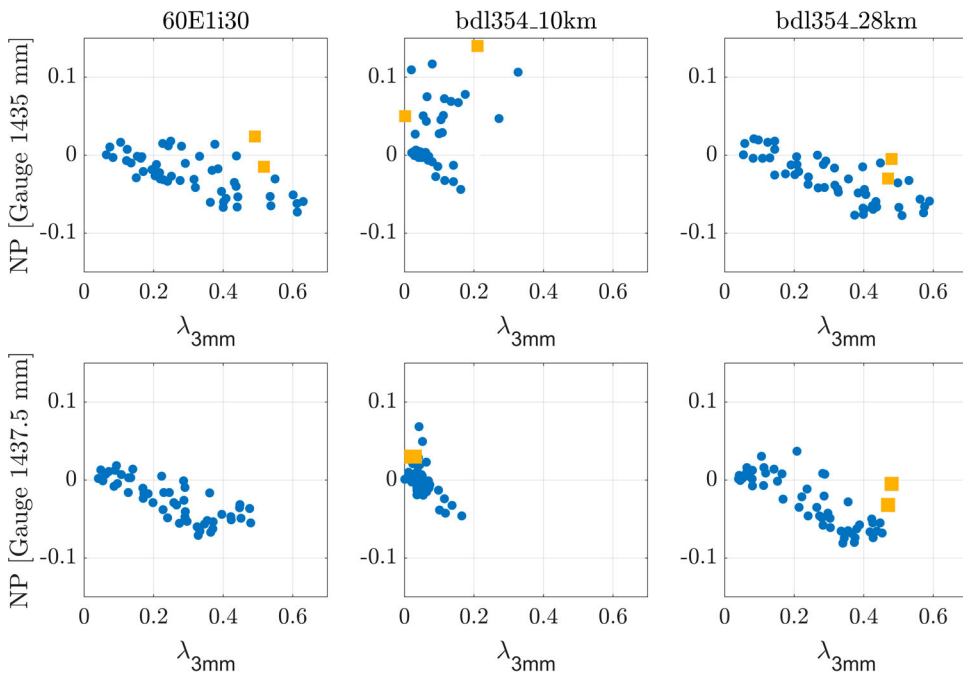


**Figure 11.** Scatter plot of equivalent conicity and NP for nominal and measured rail profiles of BDL 354 for track gauge 1435 mm (top row) and 1437.5 mm (bottom row); the green square in the three subplots of the top row show equivalent conicity and NP values of T19 and T33 wheel profiles in combination with nominal and measured rail profiles of BDL 354 as tabulated in Table 1.



increases from 0 to 0.7. This means that the worn wheel profiles in combination with the 60i30 rail profile may give rise to type B equivalent conicity function (like wheel profile T33 in the above sections), i.e. NP less than zero. These type B equivalent conicity functions will generate supercritical bifurcation behaviour of the X2000 vehicle which may cause reduction in the critical speed of the X2000 vehicle. This was also shown in the previous section where type B equivalent conicity function shows a significant reduction in the critical speed of the X2000 vehicle.

It is observed in both scatter plots corresponding to BDL354\_10 km that the equivalent conicity at 3 mm is below 0.2 and mostly concentrated at 0.1. The NP values corresponding to most of the wheel profiles are close to zero or greater than zero with a few exceptions. The reason for this is that the rail was ground to obtain a profile, more similar to the 60E2i30 nominal rail profile. Thus, it can be concluded that most of these equivalent conicity functions are of type A and the X2000 vehicle should exhibit subcritical bifurcation behaviour. The critical speed of the vehicle is much higher than the operating speed of the X2000 vehicle, so it should not run unstable during regular operation. The same is observed when the X2000 vehicle bifurcation behaviour is studied in the presence of the T19 and T33 wheel profiles in combination with the BDL354\_10 km rail profile (shown by green (grey on greyscale) solid squares in the scatter plot) results are displayed in Table 2. The critical speeds given in column (i), (ii) and (iii) are more than 300 km/h, i.e. much higher than the operating speed of the X2000 vehicle and it is very unlikely that the X2000 vehicle will run unstable during regular operation in the vicinity of the BDL354\_10 km position marker.

In contrast to BDL354\_10 km, BDL354\_28 km does show many negative NP values because the rail was milled. The scatter plots corresponding to BDL354\_28 km rail profile, where the 54 wheel profile pairs are combined with BDL354\_28 km rail profiles to exhibit  $\lambda_{3\text{mm}}$  values in the range of 0–0.7 and NP values in the range of  $-0.1$ – $0.05$ . Moreover, it is also observed that the NP value decreases from 0.05 to  $-0.1$  as the  $\lambda_{3\text{mm}}$  value increases from 0 to 0.7. This means that the worn wheel profiles in combination with BDL354\_28 km rail profile may give rise to type B equivalent conicity function, i.e. NP less than zero. These type B equivalent conicity functions will generate supercritical bifurcation behaviour of the X2000 vehicle which may cause reduction in the critical speed of the X2000 vehicle. The same is observed when the X2000 vehicle bifurcation behaviour is studied in the presence of T19 and T33 wheel profiles in combination with BDL354\_28 km rail profile (shown by green (grey on greyscale) solid squares in scatter plot). These results are also tabulated in Table 1. The X2000 vehicle model exhibits supercritical bifurcation behaviour in the presence of the T33 wheel profile which results in reduced critical speed for the X2000 vehicle and the nonlinear critical speed (column (i) in Table 2) corresponding to T33 wheel profile is 213 km/h. This means that the critical speed of the X2000 vehicle in the vicinity of BDL354\_28 km position marker may drop down to a lower speed which may be close to the operating speed of the X2000 vehicle. The same may happen in the vicinity of BDL354\_28 km position marker causing the X2000 vehicle to run unstable which can deteriorate the ride comfort for passengers on-board.

#### 4.2. BDL416

Scatter plots of equivalent conicity at 3 mm and the nonlinearity parameter for 54 pairs measured wheel profiles in combination with measured rail profiles of BDL416U are shown

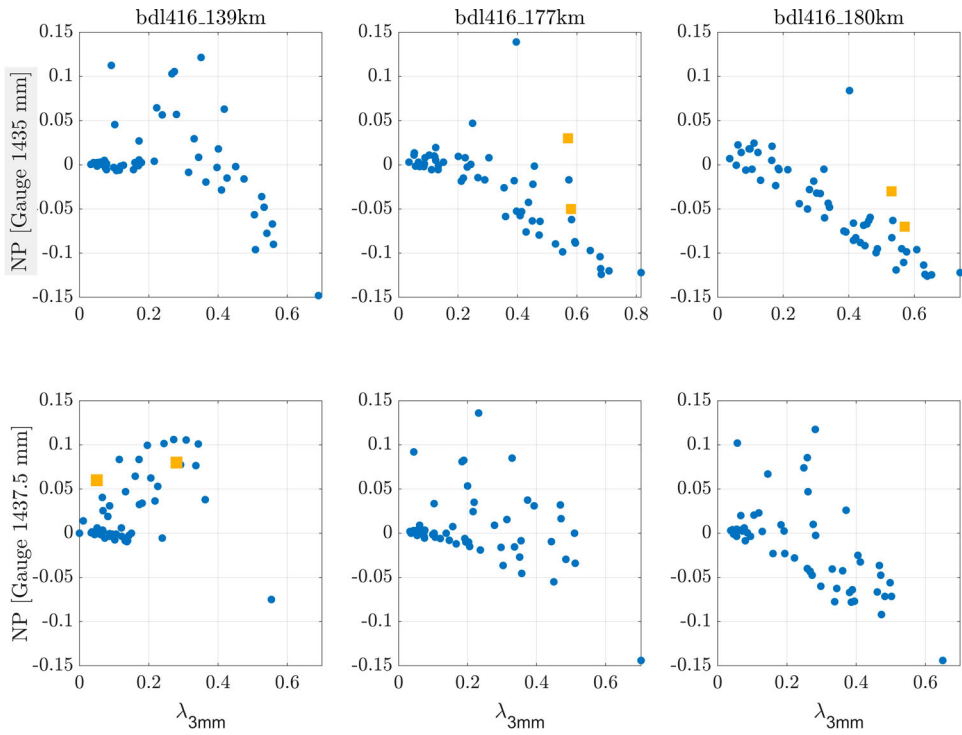


**Figure 12.** Scatter plot of equivalent conicity and NP for measured rail profiles of BDL416U for track gauge 1435 mm (top row) and 1437.5 mm (bottom row); the green square markers in three subplots show equivalent conicity and NP values of T19 and T33 wheel profiles in combination with measured rail profiles of BDL416U as tabulated in Table 2.

in Figure 12, i.e. each scatter plot contains 54 markers. The three columns correspond to measured rail profiles of the track sections at position markers of 139.105, 177.895, and 180.473 km. The important difference between rail profiles in the vicinity of 139.105 km and other two positions markers is the rail profile maintenance operation. Rail grinding is performed in the vicinity of 139.105 km, whereas rails in vicinities of 177.895 and 180.473 km are treated with milling.

It is observed in both scatter plots corresponding to BDL416\_139 km that the  $\lambda_{3mm}$  values are below 0.6 with a few exceptions which are above 0.4 when the track gauge is 1435 mm. The NP value associated with all these equivalent conicity functions is close to zero or greater than zero with a few exceptions for a track gauge of 1435 mm. The NP values corresponding to most of the wheel profiles are also close to zero or greater than zero with a few exceptions. Moreover, it is to be noted that the track gauge in the vicinity of BDL416\_139 km position marker is about 1437.5 mm; hence it is of relevance to focus on the scatter plot corresponding to the 1437.5 mm track gauge.

It is observed in the bottom-leftmost scatter plot that all equivalent conicity functions have  $\lambda_{3mm}$  in the range of 0–0.4 and corresponding NP values are in the range of 0–0.1. It can be concluded that most of these equivalent conicity functions are of type A and the X2000 vehicle should exhibit subcritical bifurcation behaviour. The critical speed of the X2000 vehicle is much higher than the operating speed. The same is observed when the

X2000 vehicle bifurcation behaviour is studied in the presence of the T19 and T33 wheel profiles in combination with the BDL416\_139 km rail profiles. The results are tabulated in Table 2. The critical speeds are given in Column (i), (ii) and (iii) are more than 270 km/h, i.e. much higher than the operating speed of the X2000 vehicle.

The scatter plots corresponding to BDL416\_177 km and BDL416\_180 km rail profiles and 54-wheel profile pairs for track gauge of 1435 and 1437.5 mm are shown in the second and third columns of Figure 12. When the track gauge is 1435 mm, all equivalent conicity functions exhibit  $\lambda_{3\text{mm}}$  values in the range of 0–0.7 and NP values in the range of –0.1–0.05, whereas when the track gauge is 1437.5 mm all equivalent conicity functions exhibit  $\lambda_{3\text{mm}}$  values in the range of 0–0.5 and NP values in the range of –0.15–0.15. Moreover, it is to be noted that the track gauge in the vicinity of BDL416\_177 km and BDL416\_180 position markers is about 1435 mm; hence it is of relevance to focus on the scatter plot corresponding to track gauge 1435 mm. It is observed in the corresponding scatter plots of BDL416\_177 km and BDL416\_180 km that the NP value decreases from 0.05 to –0.15 as  $\lambda_{3\text{mm}}$  value increases from 0 to 0.7. This means that the worn wheel profiles in combination with the BDL416\_177 km and BDL416\_180 km rail profiles may give rise to type B equivalent conicity function (like wheel profile T33 in above sections), i.e. NP less than zero. The milling operation performed in this track segment resulted in high equivalent conicity values where the track gauge is tight. These type B equivalent conicity functions will generate supercritical bifurcation behaviour of the X2000 vehicle which may cause reduction in the critical speed of the X2000 vehicle. The same is observed when the X2000 vehicle bifurcation behaviour is simulated in the presence of the T19 and T33 wheel profiles in combination with the BDL416\_177 km and BDL416\_180 km rail profiles (shown by solid green (grey on greyscale) squares in the scatter plot) and results are tabulated in Table 2. The X2000 vehicle model exhibits supercritical bifurcation behaviour in the presence of the T19 wheel profile on both rail profiles, and the same results in reduced critical speed for the X2000 vehicle. The nonlinear critical speeds (column (i) in Table 2) corresponding to T19 wheel profile in combination with BDL416\_177 km and BDL416\_180 km rail profiles are 233 and 215 km/h, respectively. This means that the critical speed of the X2000 vehicle in the vicinity of BDL416\_177 km and BDL416\_180 km position markers may drop down to a lower speed which may be close to the operating speed of the X2000 vehicle. The same may cause the X2000 vehicle to run unstable in the vicinity of BDL416\_177 km and BDL416\_180 km position markers which can deteriorate the ride comfort for passengers on-board. In fact, the poor ride comfort was measured in the vicinity of BDL416\_177 km and BDL416\_180 position markers and not in the vicinity of BDL416\_139 km position marker.

## 5. Conclusions

In this investigation, a large database of nonlinear equivalent conicity functions was obtained by combining measured wheel profile pairs of the X2000 vehicle with measured rail profile pairs from the Swedish rail network, for two track gauges (1435 and 1437.5 mm). The equivalent conicity function's nonlinearity was assessed via Polach's nonlinearity parameter (NP). The effect of the equivalent conicity function's NP value on the running stability of the X2000 vehicle was investigated by two approaches: the nonlinear critical speed identification and the safety limit method described in the EN14363 standard

under typical operating conditions. The effect of NP on the running stability of the X2000 vehicle was investigated with the help of measured wheel profiles which generates type A ( $NP > 0$ ) and type B ( $NP < 0$ ) equivalent conicity functions for the same nominal equivalent conicity ( $\lambda_{3mm}$ ) when paired with the reference rail profile 60E1i30. The conclusions of the investigation are elaborated henceforth:

- (1) The equivalent conicity functions in the database exhibited an inverse relationship between  $\lambda_{3mm}$  and NP, i.e. NP is negative ( $NP < 0$ ) for larger  $\lambda_{3mm}$  values. Thus, the X2000 vehicle assembled with heavily worn wheelsets would get subjected to type B ( $NP < 0$ ) equivalent conicity functions under high nominal conicity conditions.
- (2) The NP significantly influenced the bifurcation behaviour of the X2000 vehicle and the nonlinear critical speed. The X2000 vehicle exhibited supercritical bifurcation in the presence of type B ( $NP < 0$ ) and subcritical bifurcation in the presence of type A ( $NP > 0$ ) equivalent conicity functions, respectively. Hence, the nonlinear critical speed of the X2000 vehicle was drastically decreased in the presence of type B equivalent conicity function and was close to the regular operating speed of the vehicle. Moreover, it was also observed that the X2000 vehicle experienced larger bogie frame accelerations in the lateral direction in the presence of equivalent conicity function type B than type A, under normal operating conditions. Thus, the X2000 vehicle assembled with heavily worn wheelsets would exhibit poor dynamic behaviour because of the presence of type B equivalent conicity function and would cause deteriorated ride comfort for passengers.
- (3) NP vs.  $\lambda_{3mm}$  scatter plots corresponding to equivalent conicity functions of several measured worn wheel profiles in combination with several measured worn rail profiles of BDL354 and BDL416 track sections showed a strong prevalence of type B equivalent conicity functions among them. The X2000 vehicle model exhibited supercritical bifurcation behaviour in the presence of type B equivalent conicity function in the vicinity of BDL416\_180 km position marker. The nonlinear critical speed was, therefore, decreased down to 215 km/h which was only 15 km/h higher than the regular operating speed of the vehicle. Thus, the presence of type B equivalent conicity, deteriorated the dynamic behaviour of the X2000 vehicle and contributed to poor ride comfort while operating in the vicinity of BDL416\_180 km position marker.

The NP is obtained from the combination of wheel and rail profile pairs along with equivalent conicity ( $\lambda_{3mm}$ ). The NP associated with track can be obtained by performing conicity calculation among representative worn wheel profile pair and track rail profile pair during track measurement campaign, thus track sections susceptible for generating type B equivalent conicity functions are identified. On the other hand, NP associated with wheelsets can be obtained by using representative worn rail profile pairs while calculating the nominal wheel conicity, thus wheelsets susceptible for generating type B equivalent conicity functions are identified. Hence, the calculation of the NP is certainly useful to identify root causes of peculiar occasions of poor vehicle dynamic running and NP should be documented along with documentation of equivalent conicity ( $\lambda_{3mm}$ ). However, there is a need for further investigation to determine the precise limit values of NP which could be practically implemented for wheel, rail, and track maintenance.

## Acknowledgements

This document reflects the views of the authors and does not necessarily reflect the views or policy of the European Commission. While efforts have been made to ensure the accuracy and completeness of this document, the IN2TRACK2 consortium of Shift2Rail shall not be liable for any errors or omissions, however caused.

## Disclosure statement

No potential conflict of interest was reported by the author(s).

## Funding

This project has received funding from the European Union's Horizon 2020 research and innovation programme under Grant Agreement No 826255 (IN2TRACK2) and the Swedish Transport Administration.

## ORCID

Rohan Kulkarni  <http://orcid.org/0000-0001-5644-248X>

Alireza Qazizadeh  <http://orcid.org/0000-0002-0875-3520>

Mats Berg  <http://orcid.org/0000-0002-2571-4662>

Babette Dirks  <http://orcid.org/0000-0001-5407-2438>

Ingemar Persson  <http://orcid.org/0000-0002-6080-4938>

## References

- [1] Asplund M, Söderström P, Jönsson L-O, et al. Introduction, background and purpose of the collaboration project: a systematic approach to improve passenger ride comfort. IN2TRACK2 report. Stockholm; 2020.
- [2] S2R-IN2TRACK2 Webpage [Internet]. Available from: [https://projects.shift2rail.org/s2r\\_ip3\\_n.aspx?p=IN2TRACK2](https://projects.shift2rail.org/s2r_ip3_n.aspx?p=IN2TRACK2).
- [3] EN 15302:2008+A1 – Railway applications – Method for determining the equivalent conicity. 2010.
- [4] Technical Specification for Interoperability (TSI): 'Rolling Stock — Locomotives and passenger rolling stock' subsystem of the rail system in the European Union issued on 18 November 2014.
- [5] Technical Specifications for Interoperability (TSI): 'Infrastructure' subsystem of the rail system in the European Union issued on 18 November 2014.
- [6] Polach O. On non-linear methods of bogie stability assessment using computer simulations. *Proc Inst Mech Eng Part F J Rail Rapid Transit*. 2006;220:13–27.
- [7] Polach O. Characteristic parameters of nonlinear wheel/rail contact geometry. *Veh Syst Dyn*. 2010;48:19–36.
- [8] Mazzola L, Alfì S, Braghin F, et al. Limit wheel profile for hunting instability of railway vehicles. Grove Thomsen P, True H, editors. *Non-smooth problems in vehicle systems dynamics*. Berlin: Springer; 2010. p. 41–52.
- [9] Polach O, Nicklisch D. Wheel/rail contact geometry parameters in regard to vehicle behaviour and their alteration with wear. *Wear*. 2016;366–367:200–208.
- [10] Wei L, Zeng J, Gan F, et al. Acceptance of wheel-rail contact nonlinearity with respect to hunting stability for railway vehicles. *Proceedings of the 11th International Conference on Contact Mechanics and Wear of Rail/Wheel Systems (CM 2018)*;2018:1077–1083.
- [11] Xu K, Feng Z, Wu H, et al. Optimal profile design for rail grinding based on wheel–rail contact, stability, and wear development in high-speed electric multiple units. *Proc Inst Mech Eng Part F J Rail Rapid Transit*. 2020;234:666–677.

- [12] Polach O, Vuitton J. Which parameters determine the type of Bogie hunting bifurcation? Lecture Notes in Mechanical Engineering. Springer International Publishing, 2020.
- [13] EN 14363:2016+A1 - Railway applications – Testing and simulation for the acceptance of running characteristics of railway vehicles – Running behaviour and stationary tests. 2019.
- [14] AB DEsolver. GENSYS: A software tool for modelling and simulating vehicles running on rails [Internet]. Available from: <http://gensys.se/>.
- [15] Kalker JJ. A fast algorithm for the simplified theory of rolling contact. Veh Syst Dyn. 1982;11:1–13.
- [16] Dirks B. Vehicle dynamics simulation of wheel wear for Swedish high-speed train X2000. Stockholm: KTH Royal Institute of Technology; 2003.
- [17] EN 13674-1:2011+A1 - Railway applications – Track – Rail – Part 1: Vignole railway rails 46 kg/m and above. 2017.
- [18] EN 13715:2020 - Railway applications – Wheelsets and bogies – Wheels – Tread profile. 2020.
- [19] CEN. EN 13848-5:2017 - Railway applications – Track – Track geometry quality – Part 5: Geometric quality levels – Plain line, switches and crossings. 2017.